SUPPORTING INFORMATION

D-amino acid-mediated translation arrest is modulated by the identity of the incoming aminoacyl-tRNA

Rachel C. Fleisher, Virginia W. Cornish, and Ruben L. Gonzalez, Jr.*

Department of Chemistry, Columbia University, New York, New York 10027, USA

*To whom correspondence should be addressed: Ruben L. Gonzalez Jr., Department of Chemistry, Columbia University, 3000 Broadway, MC3126, New York, NY 10027, USA, Tel.: (212) 854-1096; Fax: (212) 932-1289; Email: rlg2118@columbia.edu

MATERIALS AND METHODS

Purification of ribosomes, translation factors, aminoacyl-tRNA (aa-tRNA) synthetases, tRNAs, and mRNAs

Tightly-coupled 70S *Escherichia coli* ribosomes were purified by sucrose density gradient ultracentrifugation using a previously described protocol[1,2]. Once purified, 70S ribosomes were stored at –80° C in a buffer containing 10 mM Tris-acetate ($pH_{25\,°C}$ = 7.5), 60 mM ammonium chloride, 7.5 mM magnesium acetate, 0.5 mM ethylenediamine tetraacetic acid (EDTA), 6mM 2-mercaptoethanol, and 40% (v/v) sucrose[2,3].

E. coli initiation factors (IFs) 1, 2, and 3; elongation factors (EF) Tu, Ts, and G; Met-$tRNA^{fMet}$ formyltransferase and Met-$tRNA^{(f)Met}$ synthetase were all purified and stored as previously described[2,4].

A Phe-$tRNA^{Phe}$ synthetase containing a six-histidine (6× His) tag at its N-terminus was purified from an overexpression strain kindly provided by Prof. David Tirrell (California Institute of Technology)[5]. Val-$tRNA^{Val}$ synthetase, Glu-$tRNA^{Glu}$ synthetase, and Arg-$tRNA^{Arg}$ synthetase overexpressing strains were kindly provided by Prof. Jack Szostak (Harvard Medical School). All four aminoacyl-tRNA synthetases were purified as previously described[6]. See the section below, entitled “Preparation of aminoacyl-tRNAs”, for a description of the procedures that were used to determine the aminoacylation efficiencies of the purified aminoacyl-tRNA synthetases.

All *E. coli* amino acid-specific tRNAs used in this study ($tRNA^{fMet}$, $tRNA^{Phe}$, $tRNA^{Val}$, $tRNA^{Arg}$, $tRNA^{Lys}$ and $tRNA^{Glu}$) were purchased in purified form from either Sigma or MP Biomedicals.

The mRNAs used here were variants of a previously described, truncated, and mutated variant of the wild-type mRNA that encodes gene product 32 from bacteriophage T4 (denoted as the $T4gp32_{1\text{-}20}$ F2K/K3F/R4E/K5V/S6Y mRNA in reference 8). Plasmids to be used as templates for *in vitro* transcription of these mRNAs were prepared using standard molecular cloning

techniques. Briefly, a pUC119-based plasmid encoding T4gp32$_{1-20}$ F2K/K3F/R4E/K5V/S6Y under the control of a T7 RNA polymerase promoter (denoted as the T4gp32$_{1-20}$ F2K/K3F/R4E/K5V/S6Y plasmid in reference 8) was used as a template for mutagenic PCR. Mutagenic PCRs were performed using nested primers containing the base pairs to be mutagenized (Table S1). Following fusion PCR assembly, the resulting PCR products were digested with restriction endonucleases EcoR1 and BamH1 and were then ligated into T4gp32$_{1-20}$ F2K/K3F/R4E/K5V/S6Y plasmid DNA that had been digested with the same restriction endonucleases so as to generate the appropriate ends for PCR product ligation. Ligated DNA was transformed into *E. coli*, single colonies were selected, and the presence of the desired mutations were verified by DNA sequencing. All mRNAs were *in vitro* transcribed using T7 RNA polymerase from linearized plasmid DNA templates following previously published, standard protocols[2,4].

Synthesis of 3,5-dinitrobenzyl active ester (DBE) and cyanomethyl active ester (CME) for acylation onto tRNAs using the 'flexizyme' system[7]

L- and D-Lys-DBE and L-Phe-CME were all used from batches that were synthesized and characterized previously[3,8].

Preparation of aminoacyl-tRNAs

We note that 'fMet' always denotes the L stereoisomer and that the stereochemistry of all other amino acids is called out explicitly. fMet-tRNA^{fMet} was prepared in a previously described, one-pot reaction in which initiator tRNA^{fMet} was aminoacylated with radiolabeled [^{35}S]-methionine (Perkin-Elmer) using Met-tRNA$^{(f)Met}$ synthetase and the resulting [^{35}S]-Met-tRNA^{fMet} was formylated using ^{10}N-formyltetrahydrofolate and Met-tRNA^{fMet} formyltransferase[2,4]. ^{10}N-formyltetrahydrofolate was prepared from folinic acid (Acros Organic) using a previously described protocol[9]. For the tripeptide synthesis reactions (described below), the second codon was decoded by an L- or D-Lys-tRNA^{Lys}. These aa-tRNAs were prepared using the 'dFx' variant

of the 'flexizyme' system developed by Suga and coworkers[7], L- or D-Lys-DBE, and $tRNA^{Lys}$ using a previously published protocol[8]. The third codon of the tripeptide synthesis reaction was decoded by any one of five different aa-tRNAs (L-Phe-$tRNA^{Phe}$, L-Arg-$tRNA^{Arg}$, L-Glu-$tRNA^{Glu}$, L-Val-$tRNA^{Val}$, and L-Phe-$tRNA^{Glu}$). Four of these aa-tRNAs (L-Phe-$tRNA^{Phe}$, L-Arg-$tRNA^{Arg}$, L-Glu-$tRNA^{Glu}$, and L-Val-$tRNA^{Val}$) were prepared using the corresponding aa-tRNA synthetase (purified as described above), amino acid, and tRNA using a previously published protocol[2,10]. The fifth L-aa-tRNA (L-Phe-$tRNA^{Glu}$) was a misacylated aa-tRNA and was prepared using the 'eFx' variant of the 'flexizyme' developed by Suga and coworkers[7], L-Phe-CME, and $tRNA^{Glu}$ using a previously described protocol[8].

The efficiency of the 'flexizyme'- or aminoacyl-tRNA synthetase-based aminoacylation reactions for $tRNA^{Lys}$, $tRNA^{Glu}$, and $tRNA^{Val}$ were determined by performing analytical-scale aminoacylation reactions using 3'-[^{32}P]-tRNAs, subsequently digesting the reaction products using P1 nuclease (Sigma), and separating and visualizing the unacylated 3'-[^{32}P]-AMP and aminoacylated 3'-aa-[^{32}P]-AMP digestion products using thin layer chromatography and phosphorimaging[8,10,11] (Fig. S1). The 3'-[^{32}P]-tRNAs were prepared by using nucleotidyl transferase (purified from an overexpressing plasmid kindly provided by Dr. Marcel Dupasquier and Prof. Ya-Ming Hou (Thomas Jefferson University) and [α-^{32}P]-ATP (Perkin-Elmer) to label the 3' termini of the tRNAs to be assessed using a previously published protocol[11].

The efficiency of the aminoacyl-tRNA synthetase-based aminoacylation reaction for $tRNA^{Arg}$ was determined using a previously published procedure in which acidic polyacrylamide gel electrophoresis was used to separate unacylated $tRNA^{Arg}$ from aminoacylated L-Arg-$tRNA^{Arg(10)}$.

The efficiency of the aminoacyl-tRNA synthetase-based aminoacylation reaction for $tRNA^{Phe}$ was determined using a previously published procedure in which hydrophobic interaction chromatography was used to separate unacylated $tRNA^{Phe}$ from aminoacylated L-Phe-$tRNA^{Phe(2)}$.

Typical aminoacylation efficiencies were ~30 % for L-Lys-DBE on $tRNA^{Lys}$, ~30 % for D-Lys-DBE on $tRNA^{Lys}$, ~95 % for L-Phe on $tRNA^{Phe}$, ~90 % for L-Arg on $tRNA^{Arg}$, ~25% for L-Glu on $tRNA^{Glu}$, ~40% for L-Val on $tRNA^{Val}$, and ~30 % for L-Phe-CME on $tRNA^{Glu}$. For aa-tRNAs prepared using either the 'flexizyme'- or aa-tRNA synthetase-based aminoacylation reactions, the aminoacylation efficiencies were used to calculate the final concentrations of aa-tRNA that were used in the tripeptide synthesis reactions.

Tripeptide synthesis reactions

General scheme

Tripeptide synthesis reactions were performed following a previously published protocol with minor modifications[8]. For each pair of fMet-L-Lys-L-X and fMet-D-Lys-L-X tripeptide synthesis reactions in which the 'X' denotes the identity of the third L-amino acid, four separate reaction mixtures were prepared: a translation initiation reaction mixture, an L-Lys EF-Tu(GTP)aa-tRNA reaction mixture, a D-Lys EF-Tu(GTP)aa-tRNA reaction mixture and an EF-G reaction mixture. The general experimental scheme was as follows: (i) A translation initiation reaction mixture was prepared in which ribosomal initiation complexes carrying an f-[^{35}S]-Met-$tRNA^{fMet}$ at the ribosomal peptidyl-tRNA binding (P) site are assembled on an mRNA encoding an fMet-Lys-X tripeptide. (ii) The translation initiation reaction mixture was then evenly divided into two Eppendorf tubes. (iii) An EF-G reaction mixture was prepared. (iv) An L-Lys EF-Tu(GTP)aa-tRNA reaction mixture was prepared that was composed of EF-Tu(GTP)L-Lys-$tRNA^{Lys}$ and EF-Tu(GTP)L-X-$tRNA^{X}$ (where 'X' denotes the identity of the third amino acid). (v) A D-Lys EF-Tu(GTP)aa-tRNA reaction mixture was prepared that was composed of EF-Tu(GTP)D-Lys-$tRNA^{Lys}$ and EF-Tu(GTP)L-X-$tRNA^{X}$. (v) The EF-G reaction mixture was combined with each of the two tubes containing the initiation reaction mixture. (vi) Tripeptide syntheses reactions were initiated by adding the L-Lys EF-Tu(GTP)L-aa-tRNA reaction mixture to one of the tubes containing the combined translation initiation reaction mixture and EF-G reaction mixture and adding the D-Lys EF-Tu(GTP)L-aa-tRNA

reaction mixture to the second tube containing the combined translation initiation reaction mixture and EF-G reaction mixture. (vii) Tripeptide synthesis reaction products were collected at various reaction time points spanning 0–60 min. (viii) Tripeptide synthesis reaction products at each timepoint were then separated using electrophoretic thin layer chromatography (eTLC) and visualized by phosphorimaging. Further details on each step of this general scheme are provided below.

Tris-Polymix Buffer for tripeptide synthesis reactions

Tripeptide synthesis reactions were performed in a Tris-Polymix Buffer made up of 50 mM Tris-acetate ($pH_{25\ ^{\circ}C}$ = 7.5), 100 mM potassium chloride, 0.5 mM calcium acetate, 3.5 mM magnesium acetate, 5 mM ammonium acetate, 6 mM 2-mercaptoethanol, 5 mM putrescine, and 1 mM spermidine.

Preparation of translation initiation reaction mixture

16.4 µL of translation initiation reaction mixture was prepared in Tris-Polymix Buffer. Tightly coupled 70S ribosomes, IF1, IF2, IF3, and GTP were mixed and incubated at 37º C for 10 minutes (min). mRNA was then added, followed by a second incubation at 37º C for 10 min. Finally, f-[^{35}S]-Met-tRNA^{fMet} was added, followed by a third incubation at 37º C for 10 min. The 70S ribosomal initiation complexes that are formed during this reaction did not undergo any further purification prior to use and, instead, the translation initiation reaction mixture was divided into two Eppendorf tubes and stored on ice until ready for use. Note that this translation initiation reaction mixture was made fresh for each experimental run. Moreover, the concentration of Mg^{2+} was never allowed to be lower than 3.5 mM at any step. The concentrations of the components in the final translation initiation reaction mixture were as follows: [70S] = 1.28 µM, [IF1] = 1.64 µM, [IF2] = 1.64 µM, [IF3] = 1.64 µM, [GTP] = 1.09mM, [mRNA] = 4.37 µM, [fMet-tRNA^{fMet}] = 0.55µM.

EF-G reaction mixture

5 µL of EF-G reaction mixture was prepared in Tris-Polymix Buffer. EF-G, GTP, phosphoenol pyruvate (PEP) (Sigma), and pyruvate kinase (PK) (Sigma) were mixed and the mixture was immediately transferred to ice without any further incubation or purification. The resulting EF-G reaction mixture was stored on ice until ready for use. The concentrations of the components in the final EF-G reaction mixture were as follows: [EF-G] = 17.5 µM, [GTP] = 1 mM [PEP] = 3 mM, [PK] = 0.01 Unit/µL.

L-Lys and D-Lys EF-Tu(GTP)aa-tRNA reaction mixtures

7.1 µL each of L-Lys and D-Lys EF-Tu(GTP)aa-tRNA reaction mixtures were prepared in Tris-Polymix Buffer. EF-Tu, EF-Ts, PEP, PK, and GTP were mixed and incubated at 37 ºC for 1 min and then immediately cooled on ice for 1 min. The resulting mixture was then divided into two Eppendorf tubes. L-Lys-tRNA^{Phe} and L-X-tRNA^{X} (where the 'X' denotes the identity of the third L-amino acid of the tripeptide to be synthesized) were added to one tube to generate the L-Lys EF-Tu(GTP)aa-tRNA reaction mixture and D-Lys-tRNA^{Phe} and L-X-tRNA^{X} were added to the second tube to generate the D-Lys EF-Tu(GTP)aa-tRNA reaction mixture. Both tubes were then incubated at 37º C for 1 min and the resulting L-Lys and D-Lys EF-Tu(GTP)L-aa-tRNA reaction mixtures were then stored on ice until ready for use. Note that the L-Lys and D-Lys EF-Tu(GTP)L-aa-tRNA reaction mixtures were made fresh for each experimental run. The concentrations of the components in each of the final L-Lys and D-Lys EF-Tu(GTP)L-aa-tRNA reaction mixtures were as follows: [EF-Tu] = 21.9µM, [EF-Ts] = 6.6 µM, [GTP] = 825 µM, [PEP] = 2.5 mM, [PK] = 0.008 Unit/µL, [L-Lys-tRNA^{Lys} or D-Lys-tRNA^{Lys}] = 2.19 µM, [L-X-tRNA^{X}] = 2.19 µM.

Tripeptide synthesis reactions

Prior to beginning the tripeptide synthesis reaction, 1.2 µL of the EF-G reaction mixture was combined with 6.4 µL of each of the tubes containing the translation initiation reaction

mixture. Tripeptide synthesis in each of the tubes was initiated with the addition of 6.4 μL of the L-Lys EF-Tu(GTP)L-aa-tRNA reaction mixture to one tube and addition of 6.4 μL of the D-Lys EF-Tu(GTP)L-aa-tRNA reaction mixture to the second tube. Thus, pairs of tripeptide synthesis reactions using the L-Lys and D-Lys EF-Tu(GTP)L-aa-tRNA reaction mixtures were performed simultaneously. The concentrations of the components in the final tripeptide synthesis reactions were as follows: [70S ribosomes] = 0.5μM, [f-[^{35}S]-Met-tRNA^{fMet}] = 0.25 μM, [IF1] = 0.75 μM, [IF2] = 0.75 μM, [IF3] = 0.75 μM, [mRNA] = 3 μM, [EF-Tu] = 10 μM, [EF-Ts] = 3 μM, [EF-G] = 1.5 μM, [L-Lys-tRNA^{Lys} or D-Lys-tRNA^{Lys}] = 1 μM, [L-X-tRNA^{X}] = 1μM, [GTP] = 0.5 mM, [Mg^{2+}] = 3.5mM, [PEP]= 1.4mM, [PK]= 0.0045 Unit/μL. The concentrations of the components in the translation initiation reaction mixture, EF-G reaction mixture, and L-Lys and D-Lys EF-Tu(GTP)aa-tRNA reaction mixtures reported in the subsections above were all established in order to obtain these concentrations in the final tripeptide synthesis reactions. In order to ensure that tripeptide synthesis reactions had gone to completion and we were measuring true end-point yields, reaction products were collected at reaction time points spanning from 0–60 min. Each reaction time point was quenched with potassium hydroxide to a final potassium hydroxide concentration of 125 mM and approximately 0.3 μL of each quenched reaction time point was spotted onto a cellulose TLC plate (EMD). The reaction products present in each reaction time point that was spotted on the TLC plates were separated using eTLC in pyridine acetate buffer (5 % pyridine, 20 % acetic acid, pH = 2.8)[12]. eTLCs were run for 30 min at 1200 V, expect for fMet-L-Lys-Val and fMet-D-Lys-Val tripeptide synthesis reactions, which were run at 800 V for 1 hour. eTLC plates were then dried, exposed to a phosphorimaging screen overnight (GE Healthcare Life Sciences), and analyzed on a Typhoon® FLA 7000 phosphor imager (Figs. 2A and 3A).

Analysis of tripeptide synthesis reactions

The intensities of eTLC spots corresponding to di- and tripeptide products (I^{di} and I^{tri}, respectively) from the tripeptide synthesis reactions performed using L-Phe-tRNA^{Phe}, L-Glu-

$tRNA^{Glu}$, L-Arg-$tRNA^{Arg}$, and L-Phe-$tRNA^{Glu}$ were quantified using ImageQuant® software. The fraction of L-f-[^{35}S]-Met-L-Lys or L-f-[^{35}S]-Met-D-Lys dipeptide that was converted to a tripeptide (*i.e.*, the yield) at each reaction time point was calculated as a percentage using the following equation: $[(I^{tri}) / (I^{di} + I^{tri})] \times 100$. Reaction time courses were performed in duplicate for each tripeptide synthesis reaction and, for each reaction time point, the mean of the duplicate yield measurements was plotted as a function of time, with error bars representing the standard error of the mean of the duplicate yield measurements (Fig. S2). The reaction time courses demonstrate that all of the tripeptide synthesis reactions had gone to completion by 30 min. Therefore, the duplicate yield measurements of the final two reaction time points (*i.e.*, the 30 and 60 min reaction time points) from each tripeptide synthesis reaction were clustered and treated as four independent measurements of the yield. The mean yield was then calculated, with errors representing the standard deviation of the mean of the four yield measurements (Figs. S2, 2B, and 3B).

Because the fMet-L-Lys-L-Val and fMet-D-Lys-L-Val tripeptide products were challenging to fully separate from the fMet-L-Lys and fMet-D-Lys dipeptide products using our eTLC protocol, an alternative data quantification method was used to analyze the fMet-L-Lys-L-Val and fMet-D-Lys-L-Val tripeptide synthesis reactions. Here we describe the analysis of the fMet-L-Lys-L-Val tripeptide synthesis reactions, but please note that the fMet-D-Lys-L-Val tripeptide synthesis reactions were analyzed in the analogous manner. We began by using the Fiji® image processing software program to draw a line down each eTLC column containing separated reaction products and generating an intensity profile for each column[13]. The intensity profiles for all of the columns were then aligned based on the position of the peaks corresponding to the origin (*i.e.*, the position where we originally spotted the reaction) and to the unreacted f-[^{35}S]-Met amino acid. The peak corresponding to the fMet-L-Lys dipeptide product in the column containing a control fMet-L-Lys dipeptide synthesis reaction (labeled 'Dipeptide' in Figure 2A) was fit with a single Gaussian

distribution function to determine the location and width of the peak corresponding to the fMet-L-Lys dipeptide product. The peaks corresponding to the overlapping fMet-L-Lys dipeptide- and fMet-L-Lys-L-Val tripeptide products in the columns containing the fMet-L-Lys-L-Val tripeptide synthesis reactions were then fit to two Gaussian distribution functions using the non-linear least squares method. The location and width of one of these Gaussian distribution functions (denoted as the 'fMet-L-Lys Gaussian') were fixed to the location and width of the single Gaussian distribution function to which the fMet-L-Lys dipeptide product peak in the control fMet-L-Lys dipeptide synthesis reaction was fit, whereas the height of the fMet-L-Lys Gaussian distribution function was allowed to vary. In contrast, the location, width, and height of the second Gaussian distribution function (denoted as the 'fMet-L-Lys-L-Val Gaussian') were all allowed to vary. The fraction of fMet-L-Lys dipeptide converted to fMet-L-Lys-L-Val tripeptide was then calculated using the following equation: $[A^{tri} / (A^{di} + A^{tri})] \times 100$, where A^{di} is the area under the fMet-L-Lys Gaussian and A^{tri} is the area under the fMet-L-Lys-L-Val Gaussian.

SUPPORTING FIGURES

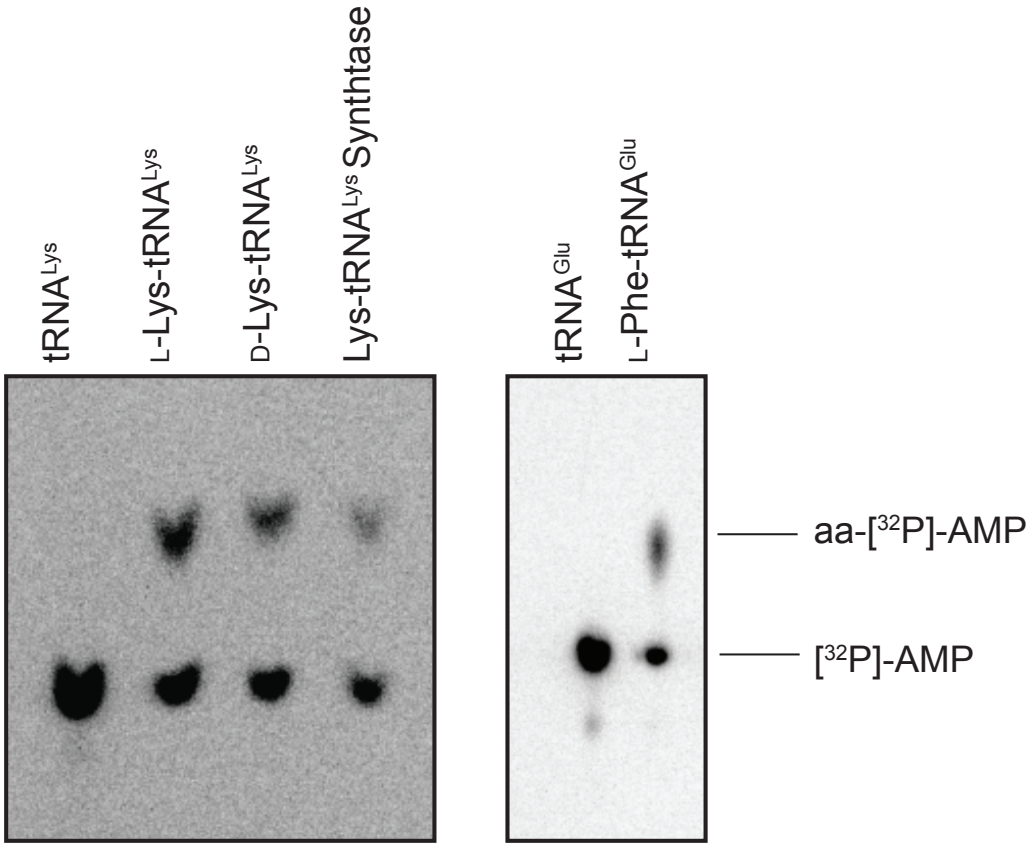

Figure S1. TLC-based separation of the [^{32}P]-AMP and aa-[^{32}P]-AMP products that were used to calculate the efficiency of the 'flexizyme' aminoacylation reactions. The efficiencies with which tRNA^{Lys} was aminoacylated with L-Lys-DBE or D-Lys-DBE and with which tRNA^{Glu} was aminoacylated with L-Phe-CME using the 'dFx' (tRNA^{Lys}) or 'eFx' (tRNA^{Glu}) variants of the 'flexizyme' developed by Suga and coworkers were determined using a previously published protocol that generates [^{32}P]-AMP and aa-[^{32}P]-AMP products that reflect the extent to which the tRNA was aminoacylated (Refs. 8, 10, 11 and SI Materials and Methods). [^{32}P]-AMP and aa-[^{32}P]-AMP products were separated using TLC and visualized on the TLC plates using

phosphorimaging. The intensities of the TLC spots corresponding to the [^{32}P]-AMP and aa-[^{32}P]-AMP products ($I^{[32P]AMP}$ and $I^{aa\text{-}[32P]AMP}$, respectively) were quantified using the ImageQuant® image processing software. The aminoacylation efficiencies, which were calculated as [($I^{aa\text{-}[32P]\text{-}AMP}$) / ($I^{[32P]AMP} + I^{aa\text{-}[32P]\text{-}AMP}$)] × 100, were 28 % for L-Lys-tRNA^{Lys}, 28 % for D-Lys-tRNA^{Lys}, and 31 % for L-Phe-tRNA^{Glu}. As a comparison, the aminoacylation efficiency with which tRNA^{Lys} was aminoacylated with L-Lys using L-Lys-tRNA^{Lys} synthetase was 21% (last column of the TLC plate on the lefthand side of the figure).

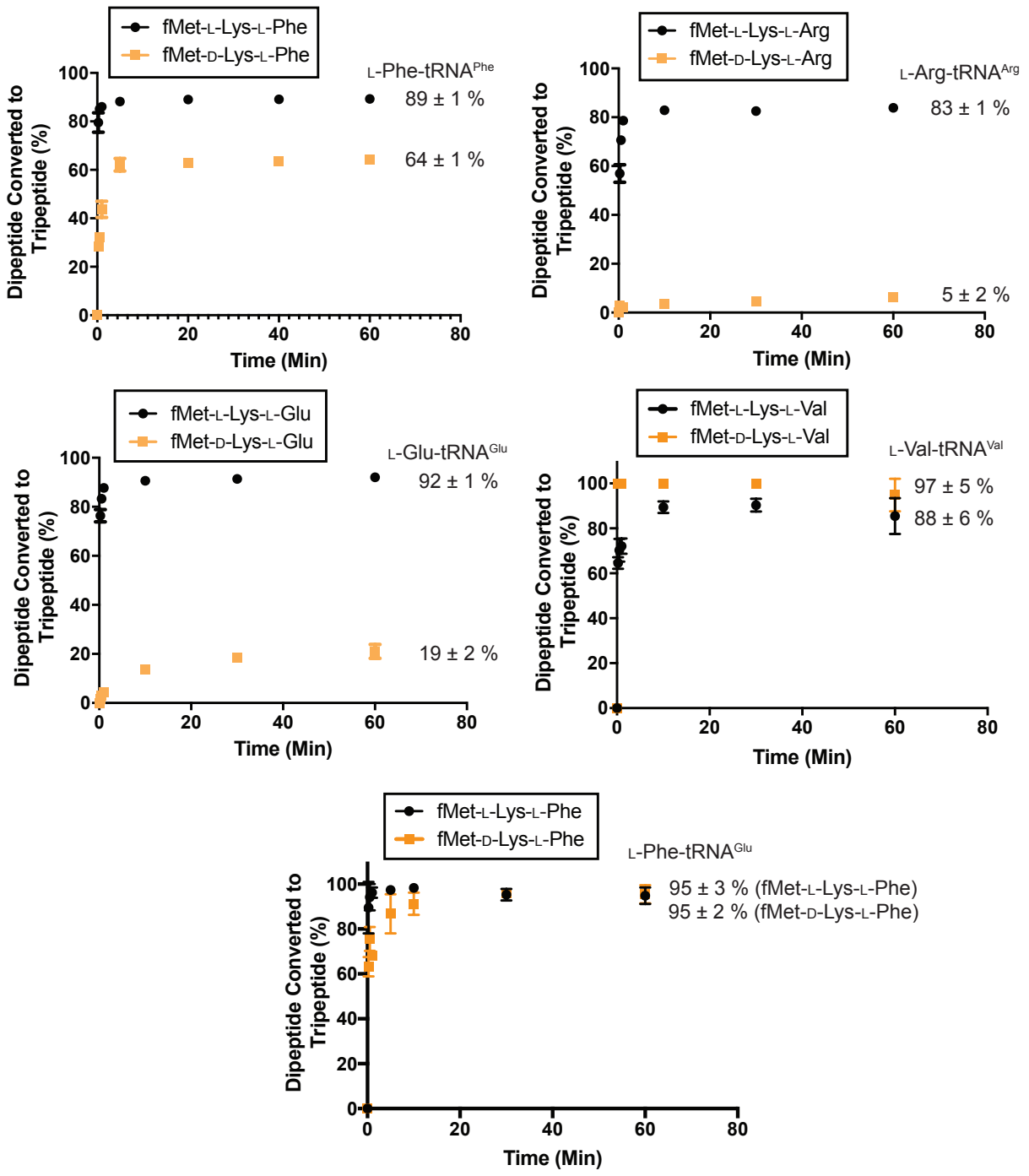

Figure S2. Tripeptide synthesis reaction time courses. The fraction of f-[^{35}S]-Met-L-Lys or f-[^{35}S]-Met-D-Lys dipeptide that was converted to a tripeptide (*i.e.*, the yield) at each reaction time point *versus* time was plotted for each tripeptide synthesis reaction using GraphPad Prism 7©. The identity of the aa-tRNA acceptor that was encoded by the third mRNA codon position is

denoted on the upper right-hand corner of each plot. Tripeptide synthesis reaction time courses were performed in duplicated and the mean of the duplicate yield measurements at each reaction time point was plotted as a function of time, with error bars representing the standard error of the mean of the duplicate yield measurements. Given that all of the tripeptide synthesis reactions had gone to completion by 30 min, the duplicate yield measurements of the final two reaction time points (*i.e.*, the 30 and 60 min reaction time points) from each tripeptide synthesis reaction were clustered and treated as four independent measurements of the yield. The mean yield was then calculated, with errors representing the standard deviation of the mean of the four yield measurements (see also Figs. 2B and 3B).

SUPPORTING TABLES

Table S1. Primers for mutagenic PCR reactions that were used to generate the T4gp32$_{1-20}$ F2K/K3F/R4E/K5V/S6Y-derived plasmids to be used as templates for *in vitro* transcription of the mRNAs used in this study.

Primer name	Restriction endonuclease	Sequence	Mutations
pUC119 forward (outside primer)		GCC AGG GTT TTC CCA GTC ACG AC	N/A
pUC119 reverse (outside primer)		CAC AGG AAA CAG CTA TGA CCA TGA TTA C	N/A
fMet-Lys-Phe-Pro forward	EcoR1	CAC AGG GCC CTA AGG AAA TAA AAA TG **AAA TTT** C CTA AAT CTA CTG CTG AAC TCG CTG C	**AAA TTT**
fMet-Lys-Phe-Pro reverse	BamH1	GCA GCG AGT TCA GCA GTA GAT TTA GGA AAT TTC ATT TTT ATT TCC TTA GGG CCC TGT G	
fMet-Lys-Arg-Pro forward	EcoR1	CAC AGG GCC CTA AGG AAA TAA AAA TG **AAA CGT** C CTA AAT CTA CTG CTG AAC TCG CTG C	**AAA CGT**
fMet-Lys-Arg-Pro reverse	BamH1	GCA GCG AGT TCA GCA GTA GAT TTA GGA CGT TTC ATT TTT ATT TCC TTA GGG CCC TGT G	
fMet-Lys-Glu-Pro forward	EcoR1	CAC AGG GCC CTA AGG AAA TAA AAA TG **AAA GAA** C CTA AAT CTA CTG CTG AAC TCG CTG C	**AAA GAA**
fMet-Lys-Glu-Pro reverse	BamH1	GCA GCG AGT TCA GCA GTA GAT TTA GGT TCT TTC ATT TTT ATT TCC TTA GGG CCC TGT G	
fMet-Lys-Val-Pro forward	EcoR1	CAC AGG GCC CTA AGG AAA TAA AAA TG **AAA GTG** C CTA AAT CTA CTG CTG AAC TCG CTG C	**AAA GTG**
fMet-Lys-Val-Pro reverse	BamH1	GCA GCG AGT TCA GCA GTA GAT TTA GGC ACT TTC ATT TTT ATT TCC TTA GGG CCC TGT G	

REFERENCES

(1) Powers, T., and Noller, H. F. (1991) A functional pseudoknot in 16S ribosomal RNA. *EMBO J. 10*, 2203–2214.

(2) Fei, J., Wang, J., Sternberg, S. H., MacDougall, D. D., Elvekrog, M. M., Pulukkunat, D. K., Englander, M. T., and Gonzalez Jr., R. L. (2010) A Highly Purified, Fluorescently Labeled In Vitro Translation System for Single-Molecule Studies of Protein Synthesis. *Methods Enzymol.*

(3) Effraim, P. R., Wang, J., Englander, M. T., Avins, J., Leyh, T. S., Gonzalez, R. L., and Cornish, V. W. (2009) Natural amino acids do not require their native tRNAs for efficient selection by the ribosome. *Nat. Chem. Biol. 5*, 947–53.

(4) Blanchard, S. C., Kim, H. D., Gonzalez, R. L., Puglisi, J. D., and Chu, S. (2004) tRNA dynamics on the ribosome during translation. *Proc. Natl. Acad. Sci. U. S. A. 101*, 12893–12898.

(5) Datta, D., Wang, P., Carrico, I. S., Mayo, S. L., and Tirrell, D. A. (2002) A designed phenylalanyl-tRNA synthetase variant allows efficient in vivo incorporation of aryl ketone functionality into proteins. *J. Am. Chem. Soc. 124*, 5652–3.

(6) Shimizu, Y., Inoue, A., Tomari, Y., Suzuki, T., Yokogawa, T., Nishikawa, K., and Ueda, T. (2001) Cell-free translation reconstituted with purified components. *Nat. Biotechnol. 19*, 751–755.

(7) Murakami, H., Ohta, A., Ashigai, H., and Suga, H. (2006) A highly flexible tRNA acylation method for non-natural polypeptide synthesis. *Nat. Methods 3*, 357–359.

(8) Englander, M. T., Avins, J. L., Fleisher, R. C., Liu, B., Effraim, P. R., Wang, J., Schulten, K., Leyh, T. S., Gonzalez, R. L., and Cornish, V. W. (2015) The ribosome can discriminate the chirality of amino acids within its peptidyl-transferase center. *Proc. Natl. Acad. Sci. U. S. A. 112*, 6038–43.

(9) Dubnoff, J. S., and Maitra, U. (1971) Isolation and properties of polypeptide chain initiation factor FII from Escherichia coli: evidence for a dual function. *Proc. Natl. Acad. Sci. U. S. A. 68*, 318–23.

(10) Effraim, P. R., Wang, J., Englander, M. T., Avins, J., Leyh, T. S., Gonzalez, R. L., and

Cornish, V. W. (2009) Natural amino acids do not require their native tRNAs for efficient selection by the ribosome. *Nat Chem Biol 5*, 947–953.

(11) Ledoux, S., and Uhlenbeck, O. C. (2008) [3'-32P]-labeling tRNA with nucleotidyltransferase for assaying aminoacylation and peptide bond formation. *Methods 44*, 74–80.

(12) Weinger, J. S., Parnell, K. M., Dorner, S., Green, R., and Strobel, S. A. (2004) Substrate-assisted catalysis of peptide bond formation by the ribosome. *Nat. Struct. Mol. Biol. 11*, 1101–6.

(13) Schindelin, J., Arganda-Carreras, I., Frise, E., Kaynig, V., Longair, M., Pietzsch, T., Preibisch, S., Rueden, C., Saalfeld, S., Schmid, B., Tinevez, J.-Y., White, D. J., Hartenstein, V., Eliceiri, K., Tomancak, P., and Cardona, A. (2012) Fiji: an open-source platform for biological-image analysis. *Nat. Methods 9*, 676–682.